UCRL-JC-129769
PREPRINT

Polarization Smoothing for the National Ignition Facility

J. E. Rothenberg

This paper was prepared for submittal to the
Third Annual International Conference on
Solid State Lasers for Application (SSLA)
to Inertial Confinement Fusion (ICF)
Monterey, California
June 7-12, 1998

August 13, 1998

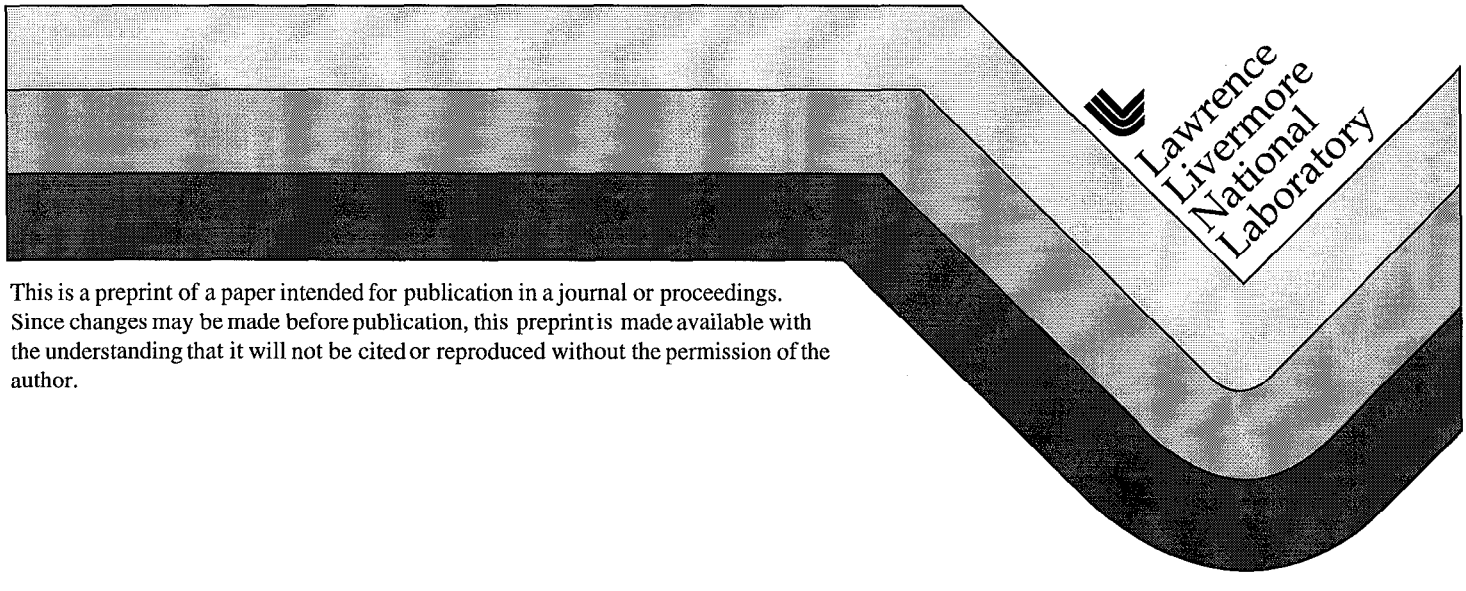

Polarization Smoothing for the National Ignition Facility

Joshua E. Rothenberg

Lawrence Livermore National Laboratory, L-441, P. O. Box 808, Livermore, CA 94551
Telephone: (510) 423-8613 , FAX: (510) 422-4982 , Email: JR1 @ LLNL.GOV

ABSTRACT

Polarization smoothing (PS) is the illumination of the target with two distinct and orthogonally polarized speckle patterns. Since these two polarizations do not interfere, the intensity patterns add incoherently and thus the contrast of the intensity nonuniformity can be reduced by a factor of $\sqrt{2}$ in addition to any reduction achieved by temporal smoothing techniques. Smoothing by PS is completely effective on an instantaneous basis and is therefore of particular interest for the suppression of laser plasma instabilities, which have a very rapid response time. The various implementations of PS are considered and their impact, in conjunction with temporal smoothing methods, on the spatial spectrum of the target illumination is analyzed.

Keywords: Beam smoothing, smoothing by spectral dispersion, inertial confinement fusion, laser plasma instabilities.

1. INTRODUCTION

Achievement of inertial confinement fusion with the upcoming megajoule-scale laser facilities using either the direct or indirect drive approaches requires a high degree of uniformity in the intense laser light focused onto the target.[1,2] A number of approaches have been proposed for reducing the nonuniformities of the intensity at focus.[3-13] A scheme that is well suited for solid-state lasers employs a random phase plate (RPP) to homogenize the long scale structure of the focal spot, and then reduces the residual fine scale speckle within the focal envelope by the smoothing by spectral dispersion (SSD) method.[4] With SSD and other temporal smoothing methods, from a time domain viewpoint, the speckle pattern in the focal plane changes at a rate determined by the total laser bandwidth, and thus the time-integrated intensity delivered to the target is smoothed. If this rate is sufficiently rapid in comparison to the response time of the target, then one expects the smoothing to be effective.[2] However, this rate is bounded by practical limits on the maximum laser bandwidth, and therefore an alternative or complementary technique is desirable.

The essential ingredient required to smooth the speckle structure in these techniques is the incoherent addition of distinct speckle patterns. In such a case, the contrast of the sum of the intensities of N distinct speckle patterns follows Gaussian statistics and will be reduced by a factor of $1/\sqrt{N}$.[12] Since the intensities of two orthogonal polarizations add incoherently, PS can effectively double the number of speckle patterns which are integrated by any temporal method and thus reduce the contrast on target by an additional $\sqrt{2}$. In addition, a major

distinction between PS and temporal smoothing methods is that PS acts to smooth the target illumination instantaneously. This is of particular importance when the target response time is very rapid, as is the case in the interaction of an intense laser beam propagating through the sub-critical plasma found in an indirect drive hohlraum. As a result, simulations have shown that PS is more effective than SSD for reducing filamentation in such a plasma and that the combination of PS and SSD results in even further reduction.[7] Thus, PS offers the promise of an improved safety margin for the goal of ignition in the upcoming megajoule Inertial Confinement Fusion (ICF) facilities.

There are a few techniques which have been considered for implementing polarization smoothing (PS).[8-11] In the first scheme considered a birefringent wedge is used to create two orthogonally polarized beams with a selected angular deviation.[8] In a second approach, the RPP is supplemented by an arrangement which scrambles the polarization in the near field.[9-11] This scrambler may have periodic (i.e., e.g., a checkerboard) or arbitrary zones of orthogonal or varying polarization states. It is found that all these PS techniques can reduce the nonuniformity contrast by $\sqrt{2}$ beyond that achieved by SSD. However, to achieve full effectiveness one must take care that the speckle patterns generated by PS are distinct and thus that the angular shifts associated with PS complement the angular shifts associated with SSD.[5] However, in spite of this requirement, a notable result is found in the case of the 2D SSD method[5,6], where the time to reach the asymptotic smoothing limit is generally much longer than the time scale of significance to the direct drive target. At the early integration times (≤ 1 ns) of importance to the target, PS by a wedge or scrambler with divergence small compared to that of the 2D SSD divergence can still be nearly ideally effective. In addition to the reduction in the aggregate contrast, PS can also modify the spatial frequency distribution of the speckle noise. The details of this distribution can have a large impact on ICF target performance.[1,13] Thus, it is of importance to calculate the modification of the spatial frequency distribution by a given embodiment of PS.

2. BIREFRINGENT WEDGES AND SCRAMBLERS

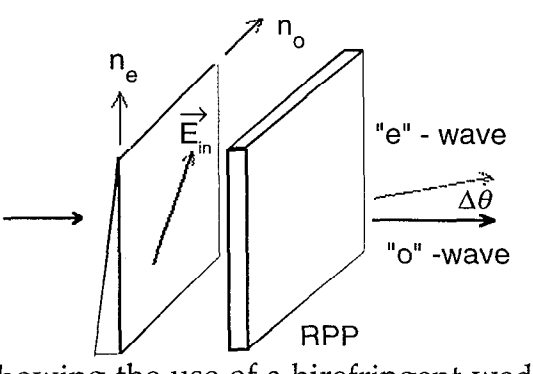

Figure 1: Schematic showing the use of a birefringent wedge to generate two shifted and orthogonally polarized speckle patterns for beam smoothing

The use of a birefringent wedge is depicted in Fig. 1. The linearly polarized beam from the conversion crystals is incident with its polarization at 45° to ordinary and extraordinary axes

of a wedged birefringent material. The birefringence causes the polarizations to be refracted into two beams separated by an angle equal to

$$\Delta\theta = \Delta n \cdot \alpha \tag{1}$$

where α is the wedge angle and Δn is the birefringence between the ordinary and extraordinary polarizations. After passage through the RPP the two polarized beams form identical speckle patterns shifted by $\Delta\theta$. The two speckle intensity patterns will incoherently add and average to reduce the intensity contrast by $\sqrt{2}$ if the speckle patterns have equal powers and are shifted sufficiently such that they are distinct. If the powers in the two polarizations P_1 and P_2 are not equal, then the reduction in the intensity contrast is given by $\sqrt{(P_1+P_2)^2/(P_1^2+P_2^2)}$. One can show that the minimum angular shift required to decorrelate a speckle pattern is the half speckle width, λ/D, where D is the square beam width[14] (e.g. the National Ignition Facility (NIF) has $D = 35$ cm, $\lambda = 351$ nm, and hence $\lambda/D = 1.0$ μrad). If one uses KDP as the birefringent material at maximum birefringence, $\Delta n = 0.045$ and the wedge angle required for the minimum 1.0 μrad shift is 23 μrad.

In a second approach the polarization is scrambled in a near field plane adjacent to the RPP. In this technique each polarization illuminates a distinct region of the RPP and thus two distinct and orthogonally polarized speckle patterns combine to illuminate the target. In this case the intensity contrast is again reduced by $\sqrt{2}$. The modification of the spatial spectrum by this technique is dependent on the type of pattern and the size of the zones used in the polarization scrambler and thus must be analyzed for each embodiment.

3. SPATIAL SPECTRUM OF A STATIC SPECKLE PATTERN

Before calculating the spatial spectra resulting from PS, recall that the spatial power spectral density of the speckle intensity from a uniformly illuminated (but randomly phased) square aperture of width D is given by[14]

$$\left|\tilde{I}(f_x,f_y)\right|^2 = \left[\Lambda(f_x/f_{\max})\Lambda(f_y/f_{\max})\Big/ f_{\max}^2 + \delta(f_x,f_y)\right]\cdot \bar{I}^2 \,, \tag{2}$$

where f_x and f_y are spatial frequencies of the speckle in the far field, $\Lambda(x) \equiv 1-|x|$ for $|x| \le 1$ and 0 for $x > 1$, $f_{\max} \equiv D/F\lambda$, F is the final focal length, $\tilde{I}(f_x,f_y)$, is the Fourier transform of the speckle intensity in the far field, $I(x_{FF},y_{FF})$, and $\bar{I} \equiv \langle I(x_{FF},y_{FF})\rangle$ denotes the average speckle intensity. The first term in Eq. (2) corresponds to the speckle noise and is referred to hereafter as the AC spatial power spectrum, and the second term is determined by the average intensity level. One can show that the AC spatial power spectrum is given by the autocorrelation of the near field intensity distribution, with the proper substitution of the far field spatial frequency variables:[14]

$$\begin{aligned}\left|\tilde{I}_{AC}(f_x,f_y)\right|^2\Big/\bar{I}^2 &= \left(I_{NF}(x,y)\otimes I_{NF}(x,y)\Big|_{x=\lambda F f_x}^{y=\lambda F f_y}\right)\div\left|\iint I_{NF}(\lambda F f_x,\lambda F f_y)\,df_x\,df_y\right|^2 \\ &= rect(x/D)rect(y/D)\otimes rect(x/D)rect(y/D)\Big|_{x=\lambda F f_x}^{y=\lambda F f_y}\Big/ f_{\max}^2 \\ &= \Lambda(f_x/f_{\max})\Lambda(f_y/f_{\max})/f_{\max}^2 \,,\end{aligned} \tag{3}$$

where x and y in this equation refer to near field coordinates, $\otimes$ denotes correlation (i.e. $a(x)\otimes b(x)\equiv\int a(x+s)b(s)ds$), $rect(x)=1$ for $|x|\le 1/2$ and 0 otherwise, and a square uniform illumination distribution has been assumed. For the rest of this analysis it will be assumed that all spatial frequencies are normalized such that $f_{\max}=1$ so that one can write

$$\left|\tilde{I}_{AC}(f_x,f_y)\right|^2\Big/\bar{I}^2=\Lambda(f_x)\Lambda(f_y)\ . \tag{4}$$

From Parseval's theorem, the square of the normalized variance is found to be simply related to the AC spatial power spectrum by the relation

$$\sigma^2\equiv\left\langle(I-\bar{I})^2\right\rangle\Big/\bar{I}^2=\iint\left|\tilde{I}_{AC}\right|^2 df_x df_y\Big/\bar{I}^2\quad , \tag{5}$$

Thus, the power spectrum of Eq. (4) has been normalized such that its integral over normalized spatial frequency gives $\sigma^2=1$, as expected for a single speckle pattern.

4. BIREFRINGENT WEDGE POLARIZATION SHIFTER

The modification of the spatial power spectrum of the far field intensity pattern owing to the birefringent wedge can now be easily quantified. Let the speckle pattern owing to a single polarization be given by $I_1(x_{FF},y_{FF})$. Assuming the wedge disperses the two polarizations by an angle $\Delta\theta$ along the x direction, its effect is to generate two such patterns shifted along x the distance $\Delta x_{FF}=\Delta\theta\cdot F$. Since there is no interference between the orthogonal polarizations one can write the total intensity on the target as

$$I_{total}(x_{FF},y_{FF})=I_1(x_{FF},y_{FF})+I_1(x_{FF}+\Delta x_{FF},y_{FF})=I_1(x_{FF},y_{FF})*\left[\delta(x_{FF})+\delta(x_{FF}-\Delta x_{FF})\right], \tag{6}$$

where $*$ denotes convolution (i.e. $a(x)*b(x)\equiv\int a(x-s)b(s)ds$). Thus one can now take the Fourier Transform to obtain the spatial power spectrum of the total intensity distribution

$$\begin{aligned}\left|\tilde{I}_{AC,total}(f_x,f_y)\right|^2/\bar{I}_{total}^2&=4\left|\tilde{I}_1(f_x,f_y)\right|^2\cdot\cos^2(\pi\Delta x_{FF}\cdot f_x\cdot f_{\max})/4\bar{I}_1^2\\&=\Lambda(f_x)\Lambda(f_y)\cdot\cos^2(\pi\Delta x_{FF}\cdot f_x\cdot f_{\max})\end{aligned}\quad , \tag{7}$$

where the single polarization result of Eq. (4) has been invoked. Thus, one has the intuitive result that the wedge modifies the spatial spectrum by imposing a sinusoidal modulation along the shift direction with period $1/\Delta x_{FF}$. Hence, the total speckle noise power has been reduced by a factor 2 and the intensity contrast reduced by $\sqrt{2}$.

5. REGULAR 'CHECKERBOARD' SCRAMBLER

The spatial spectrum of speckle generated by each polarization of a scrambler can be found from a simple extension of Eq. (3). Consider the simple 1D case of a scrambler consisting of N uniform regions (i.e. stripes) of polarization separated by equal regions of orthogonal polarization. Following the same analysis leading to Eq. (4) one finds that the normalized spectrum is given by

$$\left|\tilde{I}_{AC\,total}(f_x)\right|^2/\bar{I}^2=\Lambda(f_x\cdot 2N)*\left\{\textstyle\sum_{m=1-N}^{N-1}(N-|m|)\delta(f_x+m/N)\right\}/N\quad . \tag{8}$$

This result is shown (solid curve) in Fig. 2 for the case of N=8. One finds again that the scrambler reduces the total noise power (and hence also the variance σ^2) by a factor 2. This reduction is achieved owing to the lack of interference between orthogonally polarized

regions, which also leads to the periodic modulation of the spectrum shown. One finds this periodic modulation is very similar to that achieved using an appropriate birefringent wedge (see Eq. (7)). For this comparison the spectrum obtained using a birefringent wedge which produces an angular deviation between polarizations of $8 \cdot \lambda / D$ is shown by the dotted curve in Fig. 2. One sees that the spectrum obtained with this birefringent wedge is nearly identical to that of the 1D polarization scrambler. This equivalence is conceptually clear once one realizes that the wedge, in effect, causes the near field polarization to alternate between orthogonal states, just like the scrambler. For a wedge of deviation $N \cdot \lambda / D$, the polarization is orthogonal between near field positions separated by $D / 2N$, which is the same as the separation of the polarization zones in a scrambler with N pairs of alternating stripes. When compared to the static speckle spectrum (dashed curve in Fig. 2), the effect of either method is to reduce the speckle power spectrum by a factor of 2 when averaged over an interval larger than the spectral modulation period (in the case of Fig. 2, $f_{\max} / 8$).

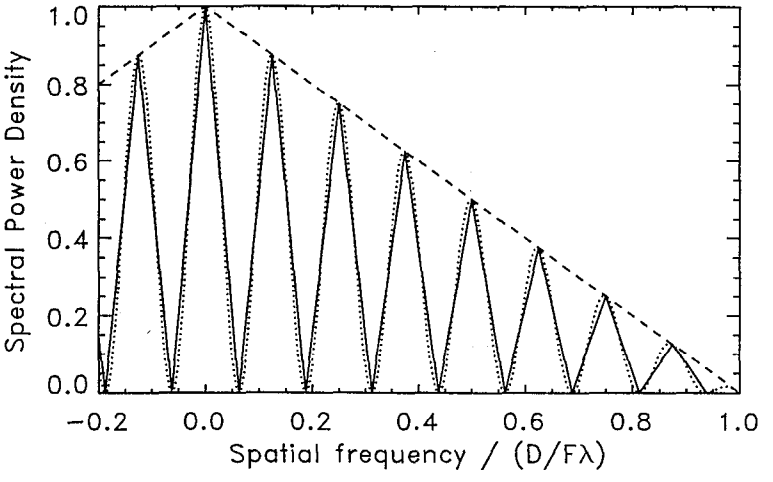

Figure 2: Spatial spectral power density along the axis of smoothing generated by a 1D scrambler with 8 pairs of alternating stripes of orthogonal polarization (solid curve). The dotted curve is the result of polarization smoothing with a birefringent wedge with an angular deviation of $8 \cdot \lambda / D$. The dashed curve is the spectrum of a static speckle pattern with no polarization scrambler.

This 1D result is easily extended to a regular two dimensional checkerboard polarization scrambler. For such a device with 2N x 2N square regions of polarization one finds

$$\left|\tilde{I}_{AC_{total}}(f_x, f_y)\right|^2 / \bar{I}^2 = \Lambda(f_x \cdot 2N)\Lambda(f_y \cdot 2N)$$
$$* \sum_{\substack{l,m=1-2N \\ l+m \text{ even}}}^{2N-1} \left[(N - |m|/2)(N - |l|/2) + (1/4)\delta_{l,m\ \text{odd}}\right]\delta(f_x + l/2N)\delta(f_y + m/2N) / N^2 \quad (9)$$

where the Kronecker function $\delta_{l,m\ \text{odd}}$ is unity when l and m are both odd and zero otherwise.

6. POLARIZATION SMOOTHING USING STRESS BIREFRINGENCE

Because of the expense and increased nonlinear effects introduced by an additional KDP optic, it is desirable to find a more practical PS implementation. One such possibility involves imposing stress to induce birefringence in an already existing optic proximal to the final focus lens. Let the near field intensity given by $I_{NF}(x,y)=|E_{NF}(x,y)|^2$ be incident upon a birefringent optic of varying retardance $\phi(x,y)$. Assume the birefringent principal axes of this optic are at 45° to the input field polarization so that the input power is equally divided between the two waves. With the birefringent axes of the optic defined to be along x and y one can write the transmitted field

$$\vec{E}=\left(\hat{x}E_{NF}(x,y)+\hat{y}E_{NF}(x,y)\exp[i\phi(x,y)]\right)/\sqrt{2}\,. \tag{10}$$

After transmission through an RPP, the spatial spectrum of far field intensity of the combined polarizations can be found using an analysis similar to that used for Eqs. (2) and (3),[14]

$$\begin{aligned}\left|\tilde{I}_{AC\,total}(f_x)\right|^2/\bar{I}^2=&\Big(I_{NF}(x,y)\otimes I_{NF}(x,y)\Big|_{x=\lambda Ff_x}^{y=\lambda Ff_y}\\ &+\Re\Big\{I_{NF}(x,y)\exp[i\phi(x,y)]\otimes I_{NF}(x,y)\exp[-i\phi(x,y)]\Big|_{x=\lambda Ff_x}^{y=\lambda Ff_y}\Big\}\Big)\,,\\ &\div\left(2\left|\iint I_{NF}(x,y)dxdy\right|^2\right)\end{aligned} \tag{11}$$

where $\Re\{\cdots\}$ refers to the real part. One also finds that the variance of the superposition of the two polarized speckle patterns is given by

$$\sigma^2=\left(1+\left|\iint I_{NF}(x,y)\exp[i\phi(x,y)]dxdy\right|^2\Big/\left|\iint I_{NF}(x,y)dxdy\right|^2\right)\Big/2\,. \tag{12}$$

Stress birefringence can be described as a differential index of refraction along the principal axes of the stress tensor $\Delta n=B(\sigma_{xx}-\sigma_{yy})$, where the photoelastic constant is given by[15] $B\cong 3.5\times10^{-12}$ m^2 / N ($\equiv n^3(q_{11}-q_{12})/2$) for fused silica,[16] and σ_{xx} and σ_{yy} are the principal stresses. Since the birefringence depends on a stress differential, it is convenient to define the shear stress $\sigma_{xy}\equiv(\sigma'_{xx}-\sigma'_{yy})/2$ in terms of the principle stresses σ'_{xx} and σ'_{yy} found in a coordinate system rotated 45°. Thus the birefringent phase retardance, in waves, along the 45° diagonals of an optic can be written

$$\Delta\phi/2\pi=\Delta n\cdot z/\lambda=2B\sigma_{xy}\cdot z/\lambda=(\sigma_{xy}/730\text{ PSI})\cdot z, \tag{13}$$

where the stress is given in units of PSI, λ is assumed to be 351 nm, and z is the plate thickness in cm. An example of an implementation of imposed stress birefringence on a square fused silica plate is depicted in Fig. 3, which also shows the induced shear stress and the resulting intensity of the transmitted light with polarization rotated orthogonal to the (vertical) input.

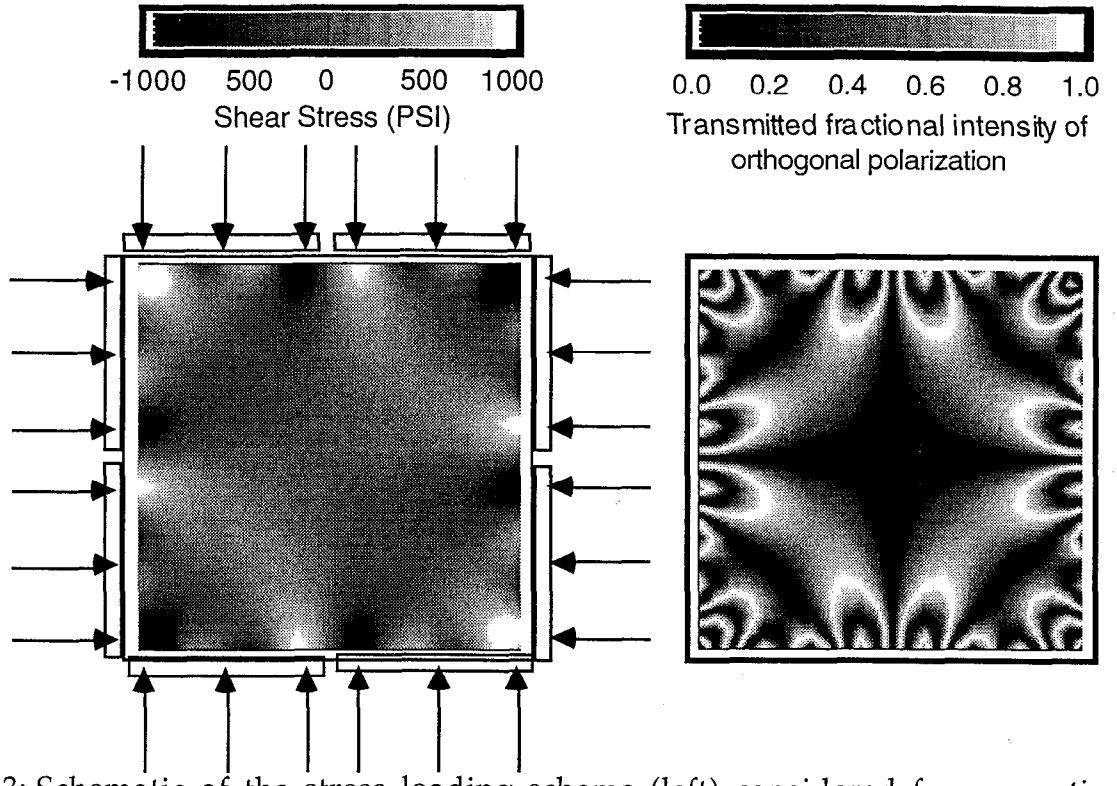

Figure 3: Schematic of the stress loading scheme (left) considered for generating highly nonuniform stress birefringence in a 42 x 42 x 1 cm fused silica plate bonded to 8 metal tabs (2 on each edge). Each tab is compressively loaded by three forces as shown. Shown inside the loading schematic is the calculated shear stress pattern for a load at each point of 2000 lbs. Right: transmission in the polarization orthogonal to the input. Fraction of the total power in the orthogonal polarization is 45 %.

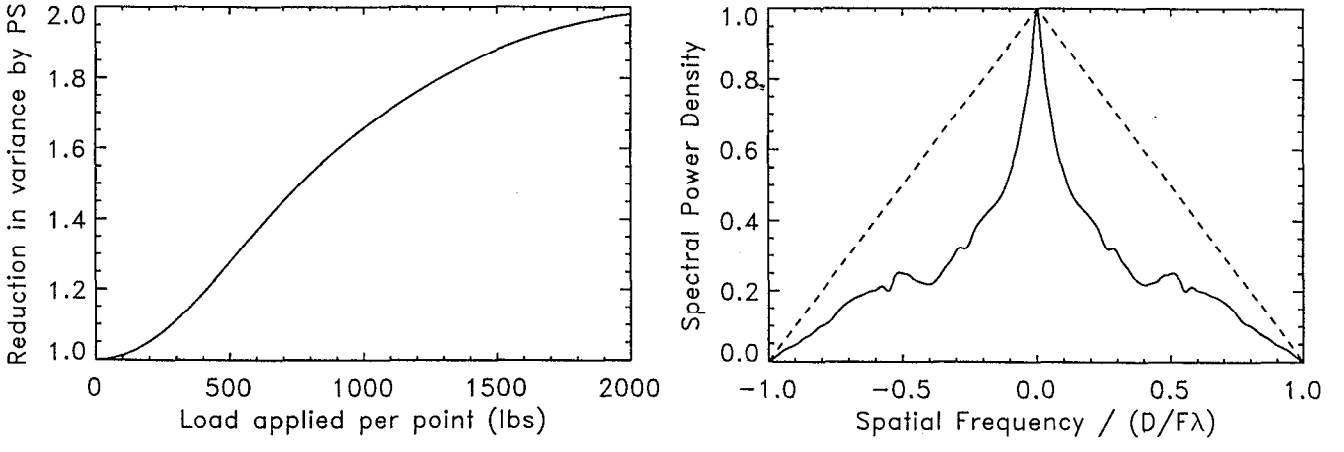

Figure 4: Left: calculated effective number of speckle patterns ($N_{eff} \equiv \sigma^{-2}$) generated by PS of a birefringent plate versus the load at each point in the design of Fig. 3. Right: spatial spectral power density along the f_x-axis of the speckle pattern generated when using the scrambler of Fig. 3 with a load at each point of 2000 lbs. The dashed curve is the spectrum of a static speckle pattern with no polarization scrambler.

In Fig. 4 the effective number of speckle patterns ($N_{eff} \equiv \sigma^{-2}$) calculated with PS using the above scheme of stress birefringence is plotted versus the loading force at each point in the design of Fig. 3. A large load (2000 lbs / point) is required to get the full reduction in σ^2 with PS of this design because of the sizable central region with low stress. The spatial spectrum was calculated along the f_x axis for a load at each point of 2000 lbs and is also shown in Fig. 4. The poor smoothing for $f_x < 0.2$ also results from the lack of PS in the central low stress region. Stress birefringence can also be imposed on an optic in a very uniform fashion and used to generate quarter- or half-wave plates in separate optics (e.g. in each of the four Beamlets which make up a group focused through a single port on the NIF) to effectively create a piecemeal 2x2 checkerboard scrambler.

7. COMBINING SSD AND POLARIZATION SMOOTHING

An important question to consider is the effect of the scrambler or birefringent wedge when used in conjunction with SSD. SSD preferentially reduces the speckle noise power at higher spatial frequency and leaves a small range of low spatial frequencies unsmoothed.[4,13] This range of unsmoothed frequencies is a result of the finite divergence of the SSD method, i.e. since the speckle motion induced by SSD is of limited extent one can not smooth spatial structure larger than this scale. Therefore it may be important in designing a polarization scrambler to ensure that it smoothes the low frequency spatial structure which has not been effectively smoothed by SSD.

An example of this consideration is shown in the calculations of Fig. 5, where the asymptotic spatial spectra of SSD without (solid curves) and with (dotted curves) PS by a birefringent wedge are compared. SSD in this calculation is assumed to have a modulation depth of 4 and thus a divergence of $\sim \pm 4 \cdot \lambda / D$, and the corresponding first nodes of the SSD spatial spectrum are seen at $\sim \pm 0.1 f_{\max}$. In Fig. 5 (a) the angular deviation induced by the wedge between the two polarizations is taken to be $8 \cdot \lambda / D$ along the dispersion direction, in which case the resultant periodic modulation of the spectrum (see Eq. (7)) has nodes at $\pm 1/16, 3/16, 5/16 \ldots \cdot f_{\max}$. Thus, one sees that the central residual power lobe of SSD is considerably narrowed by the addition of PS (dotted curve). In Fig. 5 (b), however, the wedge deviation is assumed to be only $4 \cdot \lambda / D$ and thus the corresponding nodes are at $\pm 1/8, 3/8, 5/8, \ldots \cdot f_{\max}$. As is seen in Fig. 5 (b) the central lobe is not narrowed very much. In these examples the reduction in the variance σ^2 owing to PS is 1.83 and 1.52 for Figs. 5 (a) and (b), respectively. In contrast, if the wedge deviation is larger than $10 \cdot \lambda / D$ along the dispersion direction, or at least λ / D orthogonal to the dispersion direction, then the reduction in σ^2 is found to be the maximum factor of 2.

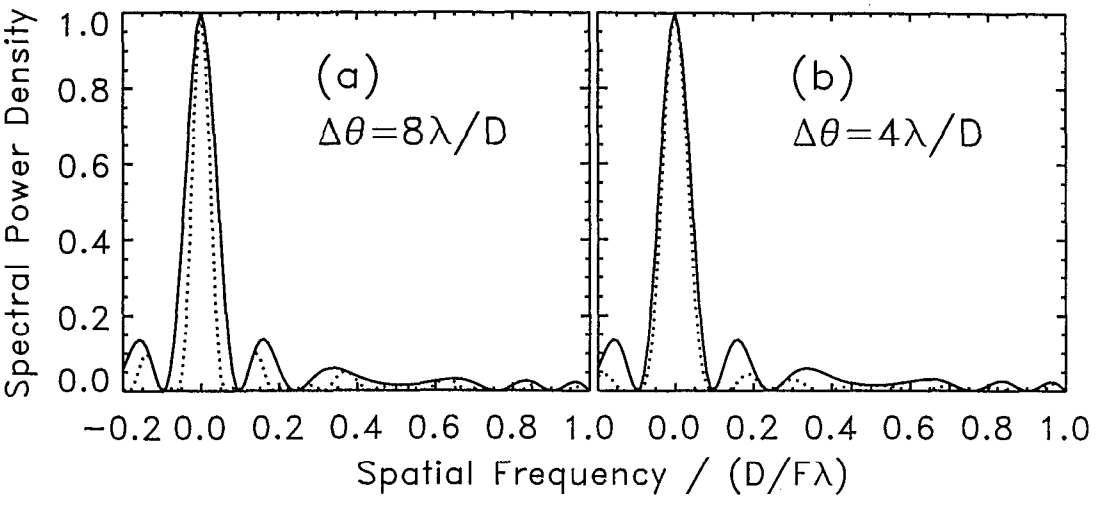

Figure 5: Spatial spectral power density along the dispersion direction of SSD with modulation depth of 4 without PS (solid curves) and with PS by a birefringent wedge (dotted curves) of deviation (a) $8 \cdot \lambda / D$ and (b) $4 \cdot \lambda / D$.

As a second example consider the effect of PS when combined with 2D SSD. The two modulation frequencies are taken to be 7 and 3 GHz, and modulation depth of 20 is assumed for each modulator. Each modulator is assumed to be critically dispersed (one color cycle - so that adjacent sidebands are separated in the far field by the angle λ / D) with the 7 and 3 GHz modulators dispersed along the x and y axes, respectively. The total UV bandwidth is then ~ 400 GHz, and the divergence is ~ $40 \cdot \lambda / D$ in each direction. Based on the discussion of 1D SSD one would think that for PS deviation $<< 40 \cdot \lambda / D$ the effectiveness of PS when combined with 2D SSD would be poor. However, because the asymptotic level of 2D SSD is not reached until a few ns, PS by a wedge at small integration times can be still quite effective even for very small angular shifts. More generally, since both 1D and 2D SSD smooth high spatial frequencies more rapidly than low ones,[13] PS by a wedge with a small shift (which provides very little smoothing at low spatial frequency) will offer little enhancement of SSD at long integration times. However, initially the aggregate variance is dominated by high spatial frequency components and thus PS is nearly ideally effective. In contrast, PS with deviation of $40 \cdot \lambda / D$ smoothes over the entire range of relevant spatial frequencies, even in the asymptotic limit. This behavior is seen in Fig. 6 which shows the reduction in the aggregate variance σ^2 by a wedge with y-deviations of 1, 2, 5, and $40 \cdot \lambda / D$ versus integration time of smoothing by 2D SSD. Thus, in the typical direct-drive ICF target physics scenario, where smoothing is most important over an integration time up to ~1 ns, one finds that the wedge deviation required for effective polarization smoothing is much less than the full 2D SSD divergence. It should be noted however, that even though at small integration times a small wedge shift may yield effective aggregate smoothing (i.e. the total contrast of the illumination nonuniformity is reduced by $\sqrt{2}$), low spatial frequencies will not be smoothed effectively, which may be of significance to the direct drive target.[1]

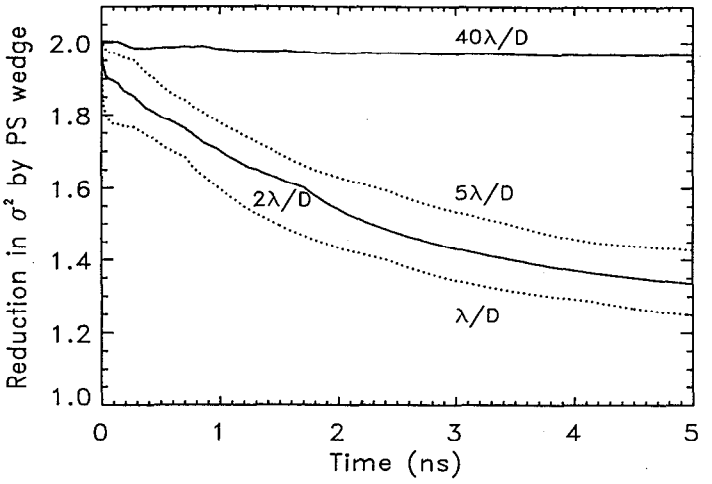

Fig. 6: Reduction in σ^2 versus integration time of 2D SSD (modulation depth 20, frequencies of 3 and 7 GHz in the x and y directions) by PS of a birefringent wedge with y-deviations of 1 (dotted), 2 (solid), 5 (dotted), and $40 \cdot \lambda / D$ (solid curve) as indicated.

8. CONCLUSIONS

It has been shown that PS by either a birefringent wedge or a scrambler can reduce the contrast of speckled target illumination by a factor of $\sqrt{2}$ beyond that achieved by SSD. The spatial spectrum resulting from PS is dependent on the spatial scale of the polarization change in the near field before focus -- smoothing of the lowest spatial frequencies thus requires change of polarization on a small scale in the near field. Equivalently this can be accomplished with a birefringent wedge of large deviation. To insure the full effectiveness of PS in the asymptotic limit, its divergence must exceed (or be orthogonal to) the divergence of the SSD. However, for 2D SSD, at the small integration times of significance to the target, a much smaller PS divergence can be nearly fully effective in reducing the aggregate contrast.

9. ACKNOWLEDGMENTS

This work was performed under the auspices of the U. S. Department of Energy by Lawrence Livermore National Laboratory under Contract No. W-7405-Eng-48. The author thanks T. Alger and C. Boley for performing the stress calculations which were used in the stress birefringence analysis.

10. REFERENCES

1. J. D. Kilkenny, S. G. Glendinning, S. W. Haan, B. A. Hammel, J. D. Lindl, D. Munro, B. A. Remington, S. V. Weber, J. P. Knauer, and C. P. Verdon, "A review of the ablative stabilization of the Rayleigh-Taylor instability in regimes relevant to inertial confinement fusion," Phys. Plasmas **1**, 1379-1389 (1994); J. E. Rothenberg, D. Eimerl, M. H. Key, and S. V. Weber, "Illumination uniformity requirements for direct drive inertial confinement fusion," Proc. Soc. Photo-Opt. Instrum. Eng. **2633**, 162-169 (1995).

2. B. J. MacGowan, B. B. Afeyan, C. A. Back, R. L. Berger, G. Bonnaud, M. Casanova, B. I. Cohen, D. E. Desenne, D. F. DuBois, A. G. Dulieu, K. G. Estabrook, J. C. Fernandez, S. H. Glenzer, D. E. Hinkel, T. B. Kaiser, D. H. Kalantar, R. L. Kauffman, R. K. Kirkwood, W. L. Kruer, A. B. Langdon, B. F. Lasinski, D. S. Montgomery, J. D. Moody, D. H. Munro, L. V. Powers, H. A. Rose, C. Rousseaux, R. E. Turner, B. H. Wilde, S. C. Wilks, and E. A. Williams, "Laser-plasma interactions in ignition-scale hohlraum plasmas" Phys. Plasmas **3**, 2029-2040 (1996).
3. R. H. Lehmberg and S. P. Obenschain, "Use of induced spatial incoherence for uniform illumination of laser fusion targets," Optics Comm. **46**, 27-31 (1983); R. H. Lehmberg and J. Goldhar, "Use of inchoerence to produce smooth and controllable irradiation profiles with KrF fusion lasers," Fusion Technology **11**, 532-541 (1987).
4. S. Skupsky, R. W. Short, T. Kessler, R. S. Craxton, S. Letzring, and J. M. Soures, "Improved laser-beam uniformity using the angular dispersion of frequency-modulated light," J. Appl. Phys. **66**, 3456-3462 (1989).
5. R. S. Craxton and S. Skupsky, "2D SSD and polarization wedges for OMEGA and the NIF," Bull. Amer. Phys. Soc. **40**, 1826 (1995).
6. J. E. Rothenberg, "Two dimensional beam smoothing by spectral dispersion for direct drive inertial confinement fusion," Proc. Soc. Photo-Opt. Instrum. Eng. **2633**, 634-644 (1995).
7. E. Lefebvre, R. L. Berger, A. B. Langdon, B. MacGowan, J. E. Rothenberg, and E. A. Williams, "Reduction of laser self-focusing in an ICF plasma by polarization smoothing," submitted to Phys. Rev. Lett, (1997).
8. "Phase conversion using distributed polarization rotation", LLE review **45**, 1-12 (1990).
9. K. Tsubakimoto, M. Nakatsuka, H. Nakano, T. Kanabe, T. Jitsuno, and S. Nakai, "Suppression of interference speckles produced by a random phase plate, using a polarization control plate", Opt. Commun. **91**, 9-12 (1992).
10. K. Tsubakimoto, T. Jitsuno, N. Miyanaga, M. Nakatsuka, T. Kanabe, and S. Nakai, "Suppression of speckle contrast by using polarization property on second harmonic generation", Opt. Commun. **103**, 185-188 (1993).
11. S. Pau, S. N. Dixit, and D. Eimerl, "Electro-optic control of correlations in speckle statistics", J. Opt. Soc. Am. B **11**, 1498 (1994).
12. J. W. Goodman, "Statistical properties of laser speckle patterns", in Topics in Applied Physics, J. C. Dainty ed., vol. 9, pp. 12-29, Springer-Verlag, New York, 1984).
13. J. E. Rothenberg, "A comparison of beam smoothing methods for direct drive inertial confinement fusion", J. Opt. Soc. Am. B, **14**, 1664-1671 (1997).
14. Ref. 11, pp. 35-40.
15. M. Born and E. Wolf, Principles of Optics, , (Pergamon, New York, 1980), p 705 .
16. American Institute of Physics Handbook, third edition, D. E. Gray ed., pp 6-233 - 6-236 (McGraw-Hill, New York, 19).